Hindawi
Mathematical Problems in Engineering
Volume 2022, Article ID 8501420, 11 pages
https://doi.org/10.1155/2022/8501420

Research Article

Analytical Solution for the Transient Current Induced along the Vertical Grounding Electrode

Ante Soldo and Silvestar Šesnić

FESB, University of Split, Split, Croatia

Correspondence should be addressed to Silvestar Šesnić; ssesnic@fesb.hr

Received 6 September 2021; Accepted 15 February 2022; Published 17 March 2022

Academic Editor: Fahd Jarad

The paper deals with the analysis of the Pocklington integro-differential equation in the time domain and its analytical solution for the transient current induced along the vertical grounding electrode and, as such, represents a continuation of the research pertaining to the horizontal grounding electrode previously reported by one of the authors. The electrode is excited by a current source impressed at one end of the electrode, representing the model of the lightning strike current. A novel analytical solution is derived using the Laplace transform. Results obtained with this time domain solution are compared with the results obtained via analytical solution of the corresponding Pocklington equation in the frequency domain in conjunction with inverse fast Fourier transform (IFFT). The results obtained via different methods are shown to be in a very good agreement. The results of the time domain analytical solution for the vertical electrode are also compared with the results of the time domain analytical solution for the horizontal electrode, where greater influence of earth-air interface on an induced current is observed. These procedures can be implemented as benchmarking techniques as well as tools for rapid estimation of the observed phenomena.

1. Introduction

Tall structures are, principally, very vulnerable to lightning strikes (e.g., telecommunication towers, wind turbines...) which facilitates the necessity to design and model an appropriate grounding and lightning protection systems (LPS) making this an important area in current and future scientific research [1–7]. Vertical grounding electrode is considered to be one of the essential components of realistic grounding systems, particularly for the protection of wind turbines [8]. Current induced along the vertical grounding electrode represents a quantity that can be subsequently used for determining other parameters of interest.

Time domain current induced along a thin wire structure is governed by integro-differential equation, either of Hallen or Pocklington type. These equations are usually solved using various numerical methods representing an established practice when dealing with highly complex systems [9, 10]. Analytical solutions, on the other hand, can be obtained by implementing appropriate approximations when dealing with canonical geometries [11–14]. The advantages of analytical solutions are: can be used for fast engineering assessment of the observed phenomenon; can be applied for reference purposes; can be used within hybrid approaches, where computational costs can be reduced [9]. The main drawback of any analytical model is its suitability for simplified canonical geometries.

In this paper, time domain analytical solution for the induced current governed with Pocklington integro-differential equation for vertical grounding electrode excited by a lightning strike is derived. In [15], the author has presented the analytical solution for the horizontal grounding electrode. However, the solution derived in this paper significantly differs from the one previously published. Taking into account vertical orientation of the grounding electrode, more complex Green's function is used which subsequently results in a differential equation with variable coefficients to be solved analytically. This approach ensures that the novel closed-form solution for the induced current along the vertical electrode is obtained.

Section 2 defines Pocklington integro-differential formulation for a current flowing along the vertical electrode buried into a lossy half-space and excited with a transient current source representing lightning current strike. Thin wire approximation is applied, while the influence of the ground-air interface is taken into account using a simplified reflection coefficient derived from the Modified Image Theory (MIT) [10]. In Section 3, approximation of the current distribution, Laplace transform and Cauchy residue theorem are used to derive the solution to the corresponding Pocklington equation. Furthermore, a model of an equivalent current source is defined. The obtained results are compared with the results for the analytical solution of the corresponding Pocklington equation in the frequency domain and the subsequent IFFT in Section 4. Additionally, the results obtained via analytical time domain solution for the vertical and horizontal grounding electrode, respectively, are compared. In Section 5, concluding remarks with the reference for future work are discussed.

2. Transient Model of the Vertical Grounding Electrode

Vertical grounding electrode of length L is buried in a lossy medium. Medium is characterized with electrical permittivity ε and electrical conductivity σ. The electrode is excited at one end with an equivalent current source. The geometry of the posed problem is shown in Figure 1.

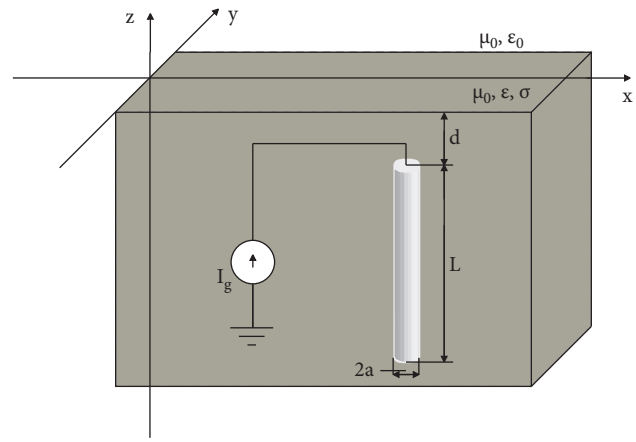

Figure 1: Vertical grounding electrode buried in a lossy half-space.

Tangential component of the total field, in the frequency domain, is equal to zero for perfectly conducting (PEC) material [15].

$$\vec{e}_z \cdot \left(\vec{E}^{inc} + \vec{E}^{sct}\right) = 0. \tag{1}$$

Since grounding electrodes are made of materials with very high conductivity, they can be considered as perfectly conducting as it is shown in [16].

Governing equation for the current induced along the electrode is derived as time-domain Pocklington integro-differential equation:

$$\left(\frac{\partial^2}{\partial z^2} - \mu\sigma\frac{\partial}{\partial t} - \mu\varepsilon\frac{\partial^2}{\partial t^2}\right) \cdot \left[\frac{\mu}{4\pi}\int_{-d}^{-d-L} I\left(z', t - \frac{R}{v}\right)\frac{e^{-1/\tau_g R/v}}{R}dz' - \frac{\mu}{4\pi}\int_0^t \int_{-d}^{-d-L} \Gamma_{ref}^{MIT}(\tau) I\left(z', t - \frac{R^*}{v} - \tau\right)\frac{e^{-1/\tau_g R^*/v}}{R^*}d\tau dz'\right] = 0. \tag{2}$$

where $I(z', t - R/v)$ represents the unknown current. Detailed derivation of (2) can be found in [17].

As can be seen in Figure 2, the distance from the source point in the wire axis to the observation point on the wire surface is defined as

$$R = \sqrt{(z - z')^2 + a^2}. \tag{3}$$

However, the distance from the source point in the image wire to the observation point on the wire surface, according to the image theory is

$$R^* = \sqrt{(z + z')^2 + a^2}. \tag{4}$$

The time constant and propagation velocity in a lossy medium depend on the properties of the medium and are given as [17]

$$\tau_g = \frac{2\varepsilon}{\sigma}, \qquad v = \frac{1}{\sqrt{\mu\varepsilon}}. \tag{5}$$

For the sake of the simplicity and considering the objective of obtaining a simple analytical solution, reflection coefficient arising from the modified image theory is used in this paper and is given as [18]

$$\Gamma_{ref}^{MIT}(t) = -\left[\frac{\tau_1}{\tau_2}\delta(t) + \frac{1}{\tau_2}\left(1 - \frac{\tau_1}{\tau_2}\right)e^{-\frac{t}{\tau_2}}\right], \tag{6}$$

where

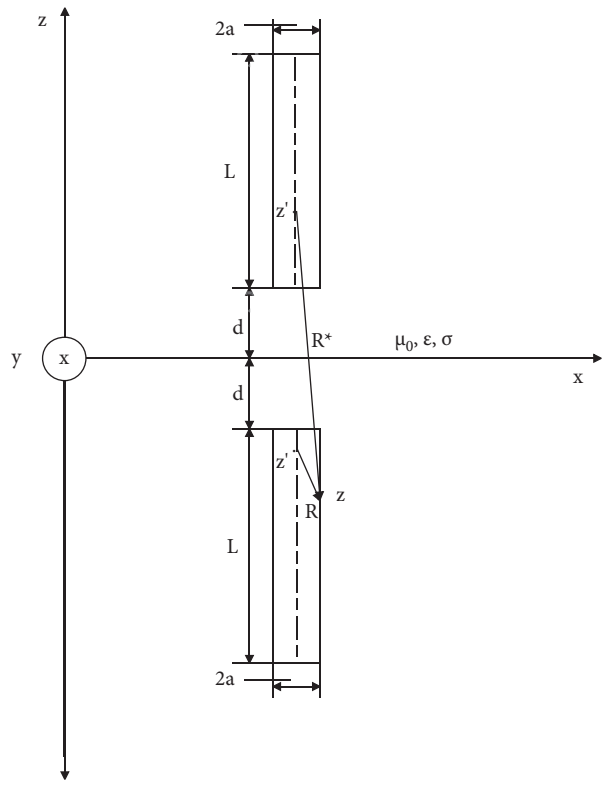

Figure 2: Vertical electrode and its image obtained by applying image theory.

$$\tau_1 = \frac{\varepsilon_0(\varepsilon_r - 1)}{\sigma}, \qquad \tau_2 = \frac{\varepsilon_0(\varepsilon_r + 1)}{\sigma}. \tag{7}$$

Reflection coefficient (6) represents the simplest characterization of the earth-air interface, taking into account only medium properties. However, an extensive validation of the application of this coefficient to thin wire problems has been carried out in [10].

3. Analytical Solution

3.1. Current Approximation. The solution for the unknown current in (2) can be obtained either by using some numerical method as in [19] or analytically using certain approximations. As it has been reported in [20, 21] and somewhat later by the authors in [17], an approximation suitable for simplifying (2) is taken as

$$\int_{-d}^{-d-L}\left(z', t - \frac{R}{v}\right)\frac{e^{-1/\tau_g R/v}}{R}\,dz'\,I = I\left(z, t - \frac{a}{v}\right)\int_{-d}^{-d-L}\frac{e^{-1/\tau_g R/v}}{R}\,dz'. \tag{8}$$

Main advantage of this approximation is simplification of the governing equation. The disadvantage is that it assumes a time retardation as a/v, which can cause some discrepancies investigated in [21].

If (2) is rewritten, it yields

$$\left(\frac{\partial^2}{\partial z^2} - \mu\sigma\frac{\partial}{\partial t} - \mu\varepsilon\frac{\partial^2}{\partial t^2}\right)\cdot\left[\frac{\mu}{4\pi}I\left(z, t - \frac{a}{v}\right)\int_{-d}^{-d-L}\frac{e^{-1/\tau_g R/v}}{R}\,dz'\right] - \frac{\mu}{4\pi}\int_0^t \Gamma_{ref}^{MIT}(\tau)I\left(z, t - \frac{a}{v} - \tau\right)\int_{-d}^{-d-L}\frac{e^{-1/\tau_g R^*/v}}{R^*}\,dz'\,d\tau = 0. \tag{9}$$

3.2. Laplace Transform and Differential Equation Solution. The transformation of the second order differential (9) into the Laplace domain is performed under the following physically justified assumptions [17].

$$I(z, t - a/v) = 0,\ t \le 0,$$
$$\frac{\partial I(z, t - a/v)}{\partial t} = 0,\ t < 0. \tag{10}$$

In the Laplace domain, (9) becomes

$$\frac{\mu}{4\pi}\left(\frac{\partial^2}{\partial z^2} - \mu\sigma s - \mu\varepsilon s^2\right) I(z,s) e^{-a/vs} \cdot \left[\int_{-d}^{-d-L} \frac{e^{-1/\tau_g R/v}}{R} dz' - \Gamma_{ref}^{MIT}(s) \int_{-d}^{-d-L} \frac{e^{-1/\tau_g R^*/v}}{R^*} dz'\right] = 0. \tag{11}$$

where $s = j\omega$ is the Laplace variable.

If the ground conductivity is equal to or less than 100 mS/m, condition [17],

$$\sigma \ll \frac{2}{a}\sqrt{\frac{\varepsilon}{\mu_0}}, \tag{12}$$

is satisfied and integrals in (11) are given with [13]

$$\Psi(z,s) = \int_{-d}^{-d-L} \frac{e^{-1/\tau_g R/v}}{R} dz' - \Gamma_{ref}^{MIT}(s) \int_{-d}^{-d-L} \frac{e^{-1/\tau_g R^*/v}}{R^*} dz' = \ln \frac{z + d + \sqrt{(z+d)^2 + a^2}}{z + d + L + \sqrt{(z+d+L)^2 + a^2}} - \Gamma_{ref}^{MIT}(s) \ln \frac{z - d - L + \sqrt{(z-d-L)^2 + a^2}}{z - d + \sqrt{(z-d)^2 + a^2}}. \tag{13}$$

Taking into account (13), (11) becomes

$$\frac{\mu}{4\pi}\left(\frac{\partial^2}{\partial z^2} - \mu\sigma s - \mu\varepsilon s^2\right) \Psi(z,s) I(z,s) e^{-a/vs} = 0. \tag{14}$$

Propagation constant is

$$\gamma = \sqrt{\mu\varepsilon\left(s^2 + \frac{\sigma}{\varepsilon} s\right)}. \tag{15}$$

Enabling the differential equation (14) to be written as follows:

$$\frac{\partial^2}{\partial z^2}\left[\Psi(z,s) I(z,s)\right] - \gamma^2 \Psi(z,s) I(z,s) = 0, \tag{16}$$

which, subsequently, leads to the second order differential equation of the form:

$$\Psi(z,s)\frac{\partial^2 I(z,s)}{\partial z^2} + 2\frac{\partial \Psi(z,s)}{\partial z}\frac{\partial I(z,s)}{\partial z} + \left[\frac{\partial^2 \Psi(z,s)}{\partial z^2} - \gamma^2 \Psi(z,s)\right] I(z,s) = 0. \tag{17}$$

Boundary conditions at the electrode ends are

$$I(-d, s) = I_g(s),$$
$$I(-d - L, s) = 0. \tag{18}$$

And, the solution of (17) is obtained

$$I(z,s) = I_g(s)\frac{\Psi(-d,s)}{\Psi(z,s)}\frac{\sinh[\gamma(z + d + L)]}{\sinh(\gamma L)}. \tag{19}$$

(19) represents current distribution in the frequency domain [22].

3.3. Cauchy Residue theorem. In order to derive the solution for the space-time distribution of the induced current, it is necessary to perform an inverse Laplace transform applying Cauchy's residue theorem [23]:

$$f(t) = \lim_{y \longrightarrow \infty} \frac{1}{j2\pi} \int_{x-jy}^{x+jy} e^{ts} F(s) \mathrm{d}s = \sum_{k=1}^{n} \mathrm{Res}(s_k), \tag{20}$$

where

$$\mathrm{Res}(s_k) = \lim_{s \longrightarrow s_k} (s - s_k) e^{ts} F(s), \tag{21}$$

while s_k represents the poles of the function $F(s)$.

Current source in the frequency domain is taken as

$$I_g(s) = 1\ [A]. \tag{22}$$

Corresponding to the impulse excitation in the time domain.

Undertaking long and tedious mathematical manipulations, the residues of current function (19) are determined according to (21) and the time domain counterpart of (19) is given as

$$I(z,t) = I_1(z) e^{ts_\Psi} + I_2(z) \cdot e^{ts_{1,2n}}. \tag{23}$$

Corresponding functions in (23) are given with

$$I_1(z) = \frac{\Psi(-d, s_\Psi)}{k \ln z - d + \sqrt{(z-d)^2 + a^2}/z - d - L + \sqrt{(z-d-L)^2 + a^2}} \frac{\sinh[\gamma_\Psi(z + d + L)]}{\sinh(\gamma_\Psi L)},$$
$$I_2(z) = \frac{2\pi}{\mu\varepsilon L^2} \sum_{n=1}^{\infty} \frac{(-1)^{n-1} n}{\pm\sqrt{b^2 - 4c_n}} \sin\frac{n\pi(z + d + L)}{L} \frac{\Psi(-d, s_{1,2n})}{\Psi(z, s_{1,2n})}. \tag{24}$$

And, coefficients can be defined as

$$\begin{aligned}
\Psi\left(-d, s_\Psi\right) &= \ln\frac{a}{L+\sqrt{L^2+a^2}} + \frac{s_\Psi\tau_1+1}{s_\Psi\tau_2+1} \\
&\quad \cdot \ln\frac{-2d-L+\sqrt{(2d+L)^2+a^2}}{-2d+\sqrt{4d^2+a^2}}, \\
s_\Psi &= \frac{h-1}{\tau_1-h\tau_2}, \\
h &= \frac{\ln z+d+\sqrt{(z+d)^2+a^2}/z+d+L+\sqrt{(z+d+L)^2+a^2}}{\ln z-d+\sqrt{(z-d)^2+a^2}/z-d-L+\sqrt{(z-d-L)^2+a^2}}, \\
k &= \frac{1}{s_\Psi\tau_2+1}\left(\tau_2\frac{s_\Psi\tau_1+1}{s_\Psi\tau_2+1}-\tau_1\right), \\
\gamma_\Psi &= \sqrt{\mu\varepsilon\left(s_\Psi^2+\frac{\sigma}{\varepsilon}s_\Psi\right)}, \\
s_{1,2n} &= \frac{1}{2}\left(-b\pm\sqrt{b^2-4c_n}\right), \\
b &= \frac{\sigma}{\varepsilon}, \\
c_n &= \frac{n^2\pi^2}{\mu\varepsilon L^2},\ n=1,2,3,\ldots, \\
\Psi\left(-d, s_{1,2n}\right) &= \ln\frac{a}{L+\sqrt{L^2+a^2}} + \frac{s_{1,2n}\tau_1+1}{s_{1,2n}\tau_2+1}, \\
&\quad \cdot \ln\frac{-2d-L+\sqrt{(2d+L)^2+a^2}}{-2d+\sqrt{4d^2+a^2}}, \\
\Psi\left(z, s_{1,2n}\right) &= \ln\frac{z+d+\sqrt{(z+d)^2+a^2}}{z+d+L+\sqrt{(z+d+L)^2+a^2}} + \frac{s_{1,2n}\tau_1+1}{s_{1,2n}\tau_2+1}, \\
&\quad \cdot \ln\frac{z-d-L+\sqrt{(z-d-L)^2+a^2}}{z-d+\sqrt{(z-d)^2+a^2}}.
\end{aligned} \tag{25}$$

(23) defines an analytical solution for the space-time distribution of the current induced along the vertical grounding electrode excited by an equivalent current source in the form of a Dirac pulse.

3.4. Equivalent Current Source. One of the most commonly used functions for representing lightning strike is a double exponential pulse [24].

$$I_g(t) = I_0\left(e^{-\alpha t}-e^{-\beta t}\right). \tag{26}$$

An analytical convolution of (23) and (26) is performed to obtain the current flowing along the vertical electrode which is given with

$$I(z,t) = I_0\left[\begin{array}{l} I_1(z)\left(\dfrac{e^{s_\Psi t}-e^{-\alpha t}}{s_\Psi+\alpha}-\dfrac{e^{s_\Psi t}-e^{-\beta t}}{s_\Psi+\beta}\right) \\ +I_2(z)\left(\dfrac{e^{s_{1,2n}t}-e^{-\alpha t}}{s_{1,2n}+\alpha}-\dfrac{e^{s_{1,2n}t}-e^{-\beta t}}{s_{1,2n}+\beta}\right)\end{array}\right]. \tag{27}$$

(27) is an expression for the space-time distribution of current flowing along the vertical grounding electrode due to a lightning strike represented with double exponential function.

4. Numerical Results

In this chapter, the results for transient response of the vertical grounding electrode excited by a lightning strike obtained directly in the time domain via (27) are presented. For the purpose of the model verification, the results are first compared with the results obtained in the frequency domain and transformed via IFFT as presented in [25]. Subsequently, the influence of different parameters on the current distribution along the vertical electrode is examined. Additionally, the comparison with the response for the horizontal electrode for the same input parameters and the same excitation pulse are presented.

4.1. Verification of the Analytical Time Domain Solution. Transient currents for the vertical electrode with radius $a = 5\,\text{mm}$, buried at depth $d = 0.5\,\text{m}$ are calculated. Two current source pulses with different parameters are considered as excitation. The parameters of $0.1/1\,\mu\text{s}$ pulse are defined as (26)

$$I_0 = 1.1043\,A,\ \alpha = 0.07924 \cdot 10^7\,\frac{1}{s},\ \beta = 4.0011 \cdot 10^7\,\frac{1}{s}. \tag{28}$$

And, for the $1/10\,\mu\text{s}$ pulse, it is given with

$$I_0 = 1.1043\,A,\ \alpha = 0.07924 \cdot 10^6\,\frac{1}{s},\ \beta = 4.0011 \cdot 10^6\,\frac{1}{s}. \tag{29}$$

The $0.1/1\,\mu\text{s}$ pulse has higher frequency content than a $1/10\,\mu\text{s}$ pulse, so it can be used to determine the effectiveness of the proposed model for stimuli with higher frequency content [24].

Figure 3 shows the results for the transient current induced in the center of the electrode calculated with (27) for $0.1/1\,\mu\text{s}$ pulse (28) and compared with the analytical result obtained in the frequency domain for the same input parameters.

It can be seen that the agreement between the results is very satisfactory, which is additionally confirmed with Figure 456 where different electrode lengths and different ground conductivities are used.

Since only limited number of results for model verification is presented, it is important to note that the authors extensively examined and determined the validity of the model for various combinations of input parameters.

4.2. Influence of Different Physical Parameters. Examining the input parameters that affect the results, the influence of the electrode length is first shown in Figure 7. Electric properties of the ground are taken as $\sigma = 1\,\text{mS/m}$ and $\varepsilon r = 10$.

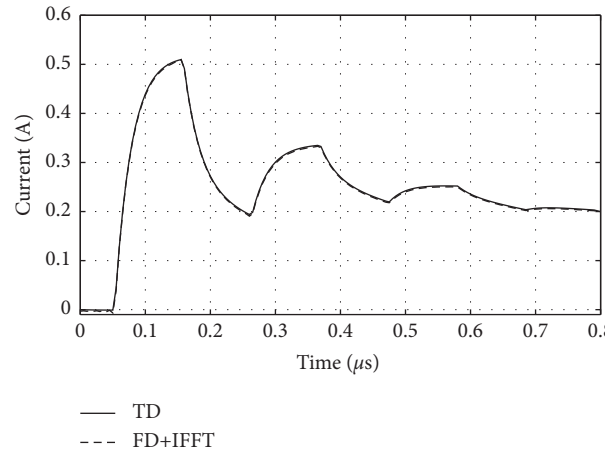

Figure 3: Current at the center of the electrode, $L = 10\,(\text{m})$; $\sigma = 1\,\text{mS/m}$.

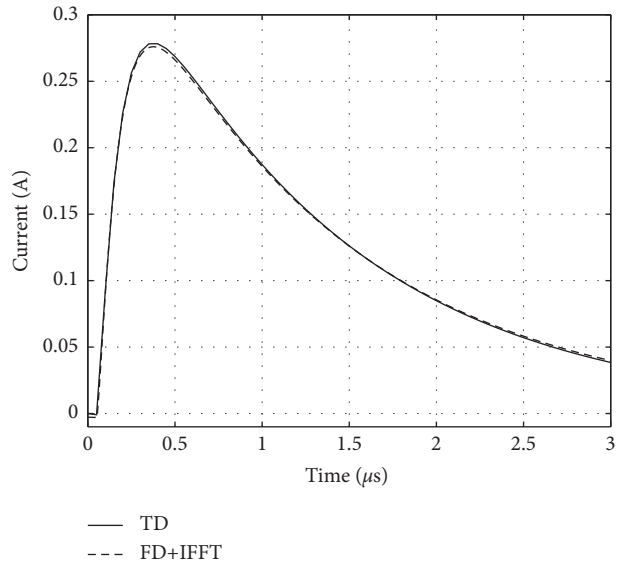

Figure 4: Current at the center of the electrode, $L = 10\,(\text{m})$; $\sigma = 10\,\text{mS/m}$.

The lightning pulse (28) is used as an excitation function in all presented results.

From the results shown in Figure 7 it can be seen that the current in the center of the electrode is equal to zero for the early time period, which is proportional to the length of the electrode and represents the time for the propagation of the current pulse from the end of the electrode where the current source is applied to its center. In the case of longer electrodes, due to the longer propagation period and the corresponding increased energy loss, the maximum value is lower.

Figure 8 shows the grounding electrode transient response for different ground conductivities. The length of the electrode is $L = 10\,\text{m}$, while electrical permittivity is $\varepsilon r = 10$. It can be seen that the decrease in the ground conductivity increases the maximum value of the current at the early time period. Additionally, the magnitude of oscillations is very

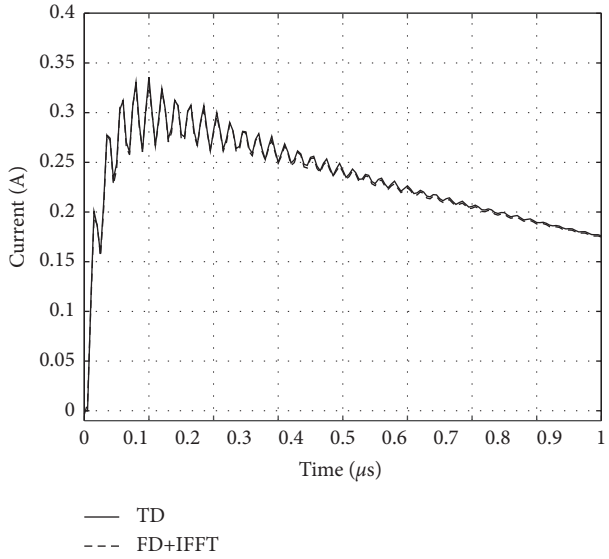

Figure 5: Current at the center of the electrode, $L = 1$ (m); $\sigma = 1$ mS/m.

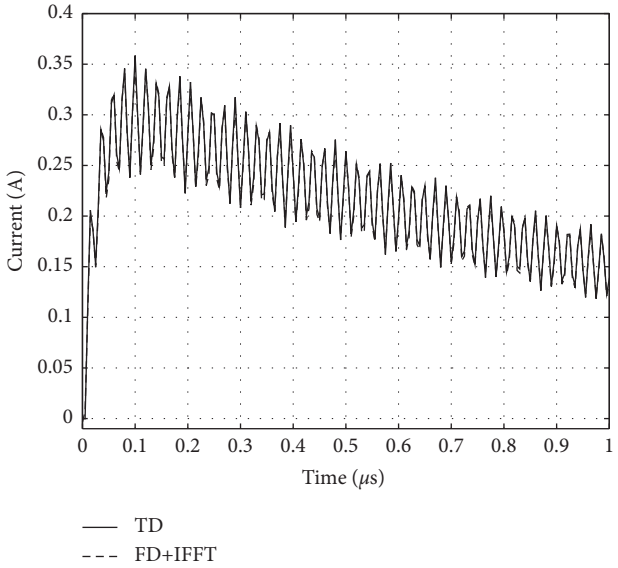

Figure 6: Current at the center of the electrode, $L = 1$ (m); $\sigma = 0.1$ mS/m.

slowly damped for low conductivity of 0.1 mS/m. Since the length of the electrode is constant, the response delay to the center of the electrode is approximately 50 ns, which shows that the conductivity of the Earth has no effect on the propagation time period.

The influence of ground permittivity is shown in Figure 9. The delay of induced current in the early time period is due to the the propagation speed in a lossy medium defined by (6) which is inversely proportional to the electrical permittivity, i.e., increasing permittivity decreases the velocity. Additionally, increasing electrical permittivity, the amplitude of the oscillations also increases, which can be explained by increasing the ratio of $\Psi(-d, s_{1,2n})$ and $\Psi(z, s_{1,2n})$ in (24).

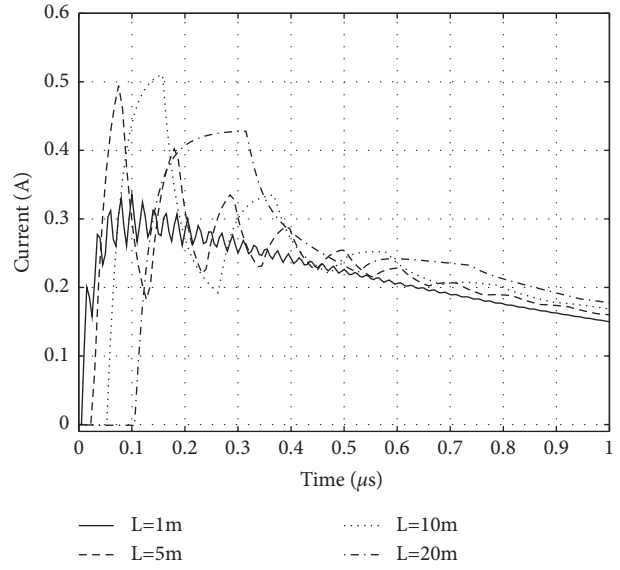

Figure 7: Current at the center of the electrode for different electrode lengths.

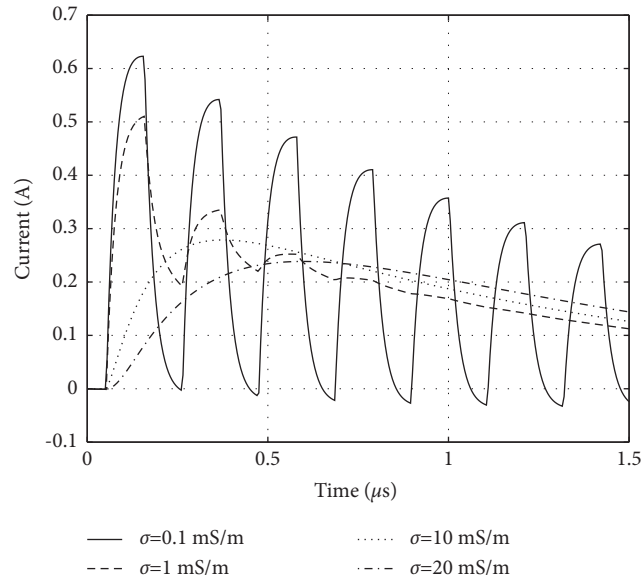

Figure 8: Current at the center of the electrode for different ground conductivities.

The results shown in Figure 10 represent transient current in the center of the vertical grounding electrode for two different electrode lengths (1 and 10 m) and for the two types of lightning current pulses (0.1/1 and 1/10 μs). For a 1/10 μs pulse, it can be seen that the current initially rises much slower than for a 0.1/1 μs pulse and that the oscillatory nature of the induced current is virtually nonexistent, which is consistent with lower frequency spectrum of the given pulse.

Figure 11 shows the space-time distribution of the current induced along the vertical grounding electrode with length $L = 10$ m, buried in the ground with electrical conductivity $\sigma = 10$ mS/m. It can be seen that the current decreases with time, as well as along the electrode.

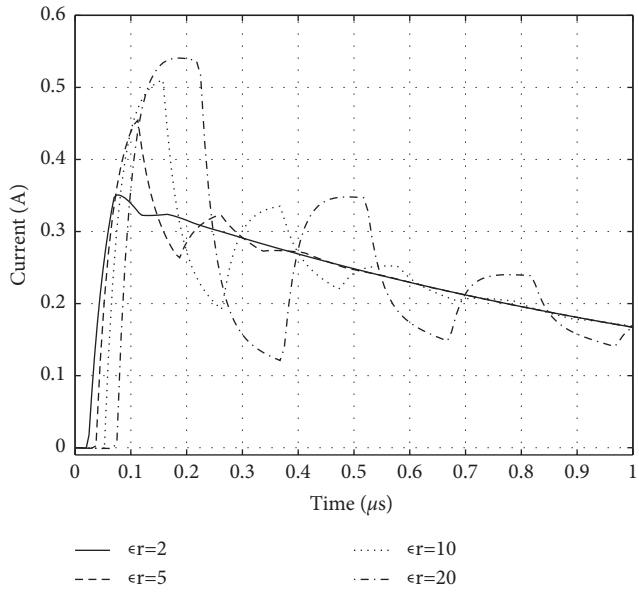

Figure 9: Current at the center of the electrode for different ground permittivity.

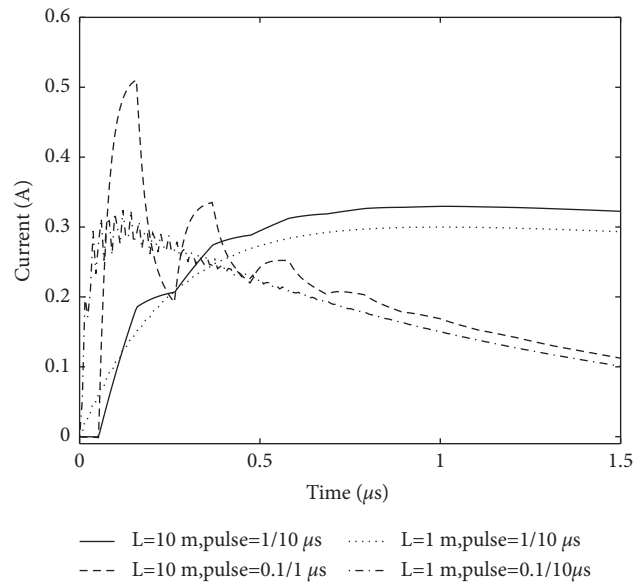

Figure 10: Current at the center of the electrode for different electrode lengths and lightning pulses.

4.3. Comparison between Vertical and Horizontal Electrode. The final set of results (Figure 12131415) show a comparison between the transient response for the induced current for vertical and the horizontal electrode [21]. The excitation pulse of 0.1/1 μs is used for both electrodes and relative dielectric permeability of the ground is $\varepsilon r = 10$. The results are shown for various values of electrode length and Earth conductivity.

Comparing the results for the transient current between the vertical and horizontal grounding electrodes, it can be seen that the waveform of the induced current is very similar for all calculated parameters, but the maximum amplitude of the induced current for the horizontal electrode is greater by approximately 35–40%. This phenomenon can be explained by the greater influence of the ground-air interface on the induced current along the horizontal electrode as oppose to the vertically buried electrode. Additionally, for the vertical electrode energy dissipation is more emphasized due to medium conductivity.

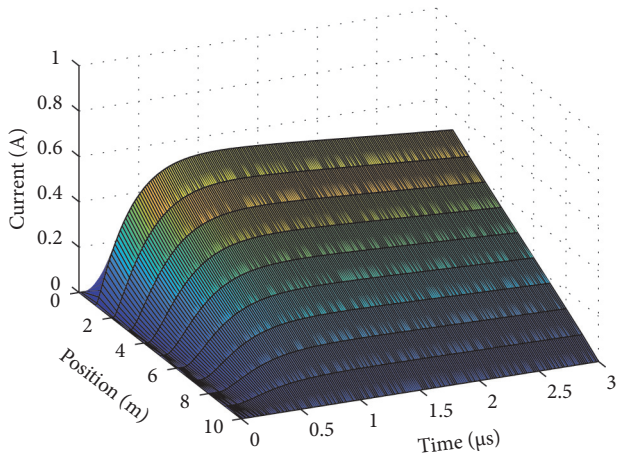

Figure 11: Current along the grounding electrode, $L = 10$ (m); $\sigma = 10$ mS/m.

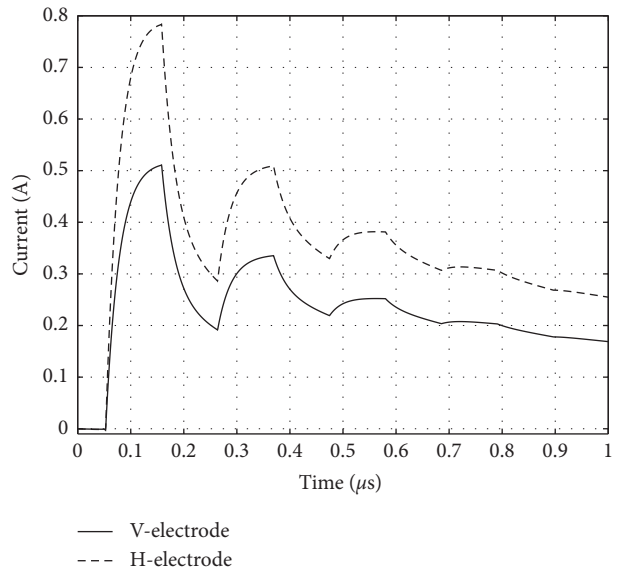

Figure 12: Comparison of transient currents for vertical and horizontal electrode, $L = 10$ (m); $\sigma = 1$ mS/m.

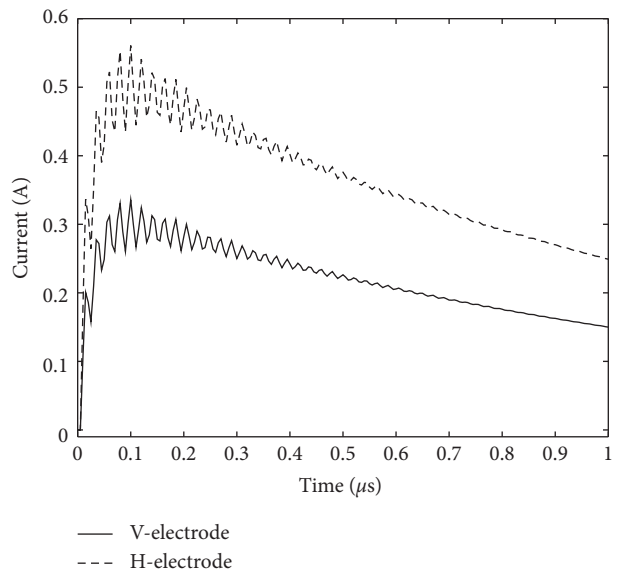

Figure 13: Comparison of transient currents for vertical and horizontal electrode, $L = 1$ (m); $\sigma = 1$ mS/m.

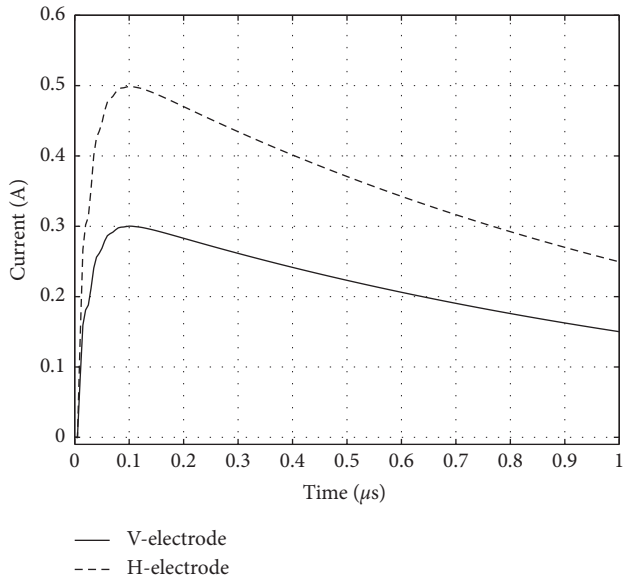

Figure 14: Comparison of transient currents for vertical and horizontal electrode, $L = 1$ (m); $\sigma = 10$ mS/m.

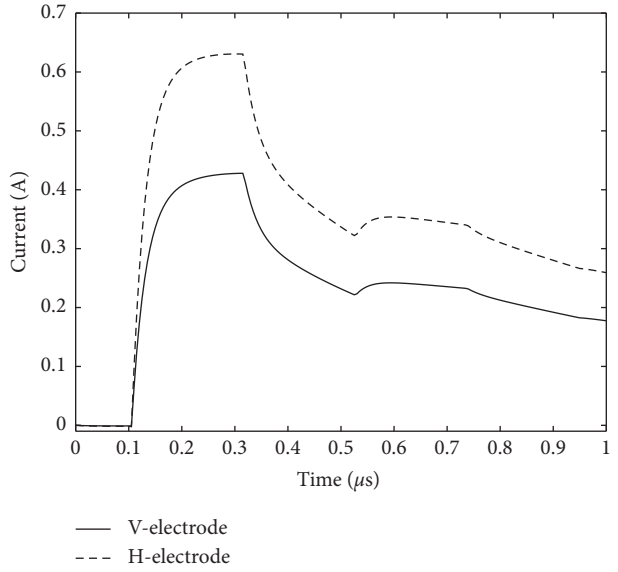

Figure 15: Comparison of transient currents for vertical and horizontal electrode, $L = 20$ (m); $\sigma = 1$ mS/m.

5. Concluding Remarks

This paper deals with the analytical solution of the Pocklington integro-differential equation in the time domain for the vertical grounding electrode. The solution is derived using an approximation of the unknown current distribution, the Laplace transform and the Cauchy residue theorem, respectively. The obtained solution represents a closed-form expression for the distribution of the induced current along the vertical electrode. The equivalent current source is used as a model of a lightning strike current excitation.

1. Results obtained in the paper are compared with the results for the analytical solution of the Pocklington equation in the frequency domain
2. The obtained results agree satisfactorily for all calculated input parameters
3. Comparison with the results for the analytical solution of the horizontal electrode obtained in the time domain is performed

Potential future work includes derivation of analytical expression for the transient scattered voltage that allows calculation of transient impedance for the vertical grounding electrode, as well as detailed Sensitivity Analysis to determine the influence of all parameters of interest.

Data Availability

Data are available on request.

Conflicts of Interest

The authors declare that they have no conflicts of interest.

References

[1] A. Meliopoulos and M. Moharam, "Transient analysis of grounding systems," *IEEE Transactions on Power Apparatus and Systems*, vol. 102, no. 2, pp. 389–399, 1983.

[2] L. Grcev and F. Rachidi, "On tower impedances for transient analysis," *IEEE Transactions on Power Delivery*, vol. 19, no. 3, pp. 1238–1244, 2004.

[3] L. Grcev, A. P. J. vanDeursen, and J. B. M. vanWaes, "Lightning current distribution to ground at a power line tower carrying a radio base station," *IEEE Transactions on Electromagnetic Compatibility*, vol. 47, no. 1, pp. 160–170, 2005.

[4] S. Visacro, "A comprehensive approach to the grounding response to lightning currents," *IEEE Transactions on Power Delivery*, vol. 22, no. 1, pp. 381–386, 2007.

[5] I. T. Report, *Wind Turbine Generation System–*, Vol. 24, Lightning Protection, Chennai, India, 2002.

[6] B. Glushakow, "Effective lightning protection for wind turbine generators," *IEEE Transactions on Energy Conversion*, vol. 22, no. 1, pp. 214–222, 2007.

[7] F. Rachidi, M. Rubinstein, J. Montanya et al., "A review of current issues in lightning protection of new-generation wind-turbine blades," *IEEE Transactions on Industrial Electronics*, vol. 55, no. 6, pp. 2489–2496, 2008.

[8] D. Cavka, D. Poljak, V. Doric, and R. Goic, "Transient analysis of grounding systems for wind turbines," *Renewable Energy*, vol. 43, pp. 284–291, 2012.

[9] D. Poljak, *Advanced Modeling in Computational Electromagnetic Compatibility*, Wiley-Interscience, New Jersey, 2007.

[10] D. Poljak and N. Kovac, "Time domain modeling of a thin wire in a two-media configuration featuring a simplified reflection/transmission coefficient approach," *Engineering Analysis with Boundary Elements*, vol. 33, no. 3, pp. 283–293, 2009.

[11] R. W. P. King, G. J. Fikioris, and R. B. Mack, *Cylindrical Antennas and Arrays*, Cambridge University Press, Cambridge, UK, 2002.

[12] R. W. P. King, "Embedded bare and insulated antennas," *IEEE Transactions on Biomedical Engineering*, vol. 24, no. 3, pp. 253–260, 1977.

[13] S. Tkatchenko, F. Rachidi, and M. Ianoz, "Electromagnetic field coupling to a line of finite length: theory and fast iterative solutions in frequency and time domains," *IEEE Transactions on Electromagnetic Compatibility*, vol. 37, no. 4, pp. 509–518, 1995.

[14] S. Tkatchenko, F. Rachidi, and M. Ianoz, "High-frequency electromagnetic field coupling to long terminated lines," *IEEE Transactions on Electromagnetic Compatibility*, vol. 43, no. 2, pp. 117–129, 2001.

[15] S. Sesnic, D. Poljak, and S. V. Tkachenko, "Analytical modeling of a transient current flowing along the horizontal grounding electrode," *IEEE Transactions on Electromagnetic Compatibility*, vol. 55, no. 6, pp. 1132–1139, 2013.

[16] D. Poljak, *Calculation of the Transient Impedance with the Proposed Design of Grounding System for Wind Turbine VE Jelinak (In Croatian)*, Split, 2010.

[17] S. Sesnic, D. Poljak, and S. V. Tkachenko, "Time domain analytical modeling of a straight thin wire buried in a lossy medium," *Progress In Electromagnetics Research*, vol. 121, pp. 485–504, 2011.

[18] T. Takashima, T. Nakae, and R. Ishibashi, "Calculation of complex fields in conducting media," *IEEE Transactions on Electrical Insulation*, vol. EI-15, no. 1, pp. 1–7, February 1980.

[19] S. M. Rao, *Time Domain Electromagnetics*, S. M. Rao, Ed., Academic Press, San Diego, CA, USA, 1999.

[20] A. G. Tijhuis, P. Zhongqiu, and A. R. Bretones, "Transient excitation of a straight thin-wire segment: a new look at an old problem," *IEEE Transactions on Antennas and Propagation*, vol. 40, no. 10, pp. 1132–1146, 1992.

[21] J. C. Bogerd, A. G. Tijhuis, and J. J. A. Klaasen, "Electromagnetic excitation of a thin wire: a traveling-wave approach," *IEEE Transactions on Antennas and Propagation*, vol. 46, no. 8, pp. 1202–1211, 1998.

[22] D. Poljak, S. Sesnic, and R. Goic, "Analytical versus boundary element modelling of horizontal ground electrode," *Engineering Analysis with Boundary Elements*, vol. 34, no. 4, pp. 307–314, 2010.

[23] J. L. Schiff, *The Laplace Transform - Theory and Applications*, Springer-Verlag, NY, USA, 1999.

[24] D. Poljak and V. Doric, "Wire antenna model for transient analysis of simple grounding systems, Part I: the vertical grounding electrode," *Progress In Electromagnetics Research*, vol. 64, pp. 149–166, 2006.

[25] D. Poljak and S. Sesnic, "Wire antenna model of the vertical grounding electrode," in *Boundary Elements and Other Mesh Reduction Methods*vol. XXXV, Brockenhurst, 2013.